PROBLEMY MECHATRONIKI
UZBROJENIE, LOTNICTWO, INŻYNIERIA BEZPIECZEŃSTWA

ISSN 2081-5891

11, 4 (42), 2020, 61-72

PROBLEMS OF MECHATRONICS
ARMAMENT, AVIATION, SAFETY ENGINEERING

Effect of Changing the Parameters of the Multi Jet Fusion (MJF) Process on the Spatial Objects Produced

Maciej CADER[1*], Wojciech KIŃSKI[2]

[1]Łukasiewicz Research Network – Industrial Institute for Automation and Measurements,
202 Jerozolimskie Ave., 02-486 Warsaw, Poland
[2]University of Warmia and Mazury in Olsztyn, Faculty of Technical Sciences,
11 Michała Oczapowskiego Str., 10-719 Olsztyn, Poland
[*]Corresponding author's e-mail address and ORCID:
maciej.cader@piap.lukasiewicz.gov.pl, https://orcid.org/0000-0003-0256-7214

Received by the editorial staff on 24 March 2020
The reviewed and verified version was received on 3 December 2020

DOI 10.5604/01.3001.0014.5644

Abstract. This paper describes the principle of operation of Multi Jet Fusion (MFJ) technology in detail. Hybrid strength tests were carried out using an INSTRON 5967 universal testing machine controlled by the Bluehill 3 program and coupled with the ARAMIS measurement system (GOM, Gmbh), enabling the monitoring of deformations in three axes, using a system of high-speed cameras. The results are given of the static tensile test of samples in two printing modes characteristic of the MJF technology – FAST and BALANCE.
Keywords: additive manufacturing**,** 3D printer, strength analysis, MJF

1. INTRODUCTION

Additive manufacturing is the most common method of producing elements for low volume production and prototyping. However, nowadays its application is much wider and can be seen, among others, in such fields as: medicine, construction, modelling, the automotive industry, fashion, the production of non-standard tools and many others [1]. One of the newest 3D printing technologies is Multi Jet Fusion (MJF), a technology developed in 2016 for additive manufacturing. It focused on speed and serial production, while maintaining a relatively high accuracy of the parts produced. For better illustration, an example from the production of a certain order has been provided. The cost of producing an injection mould with certain geometry is about PLN 40,000 and the cost of one injection is about PLN 1,50. The cost of producing 600 pieces of such parts using injection is PLN 40,900. The production time is about 5 weeks. Using the HP Multi Jet Fusion technology, the cost of producing one piece is PLN 14, i.e. the customer pays PLN 8,400 for 600 pieces. The delivery time is about 5 business days. Thus, in the context of the presented example, the client saves about PLN 32,500 and 4 weeks.

In a sense, MJF is a combination of previously known 3D printing technologies – such as Selective Laser Sintering (SLS) and PolyJet. The MJF printing process is based on layered consolidation of plastic powders. The representative material is Polyamide PA12. A specially prepared and preheated powder is applied using a roller. Thereafter, a precision printhead applies two types of adjuvant agents to the printing process. The first of them, a "fusing agent", is dispensed in model areas and its properties increase the absorption of thermal radiation. The second, a *"detailing agent"*, is applied to the outer contours of the elements to facilitate separation of unbaked powder and increase the mapping accuracy. After applying both adjuvants, a special heating head passes over the material layer, causing the model layer to melt and then the process is repeated for the next layer until the final geometry is obtained. No support structures are used.

After completion, the structure is cooled and then transferred to a processing station to remove loose powder and recycle [2]. Figure 1 shows the principle of printing operation in accordance with the assumptions of the MJF technology, while Fig. 2 shows the quality of external surfaces of the manufactured parts compared with two representative production methods.

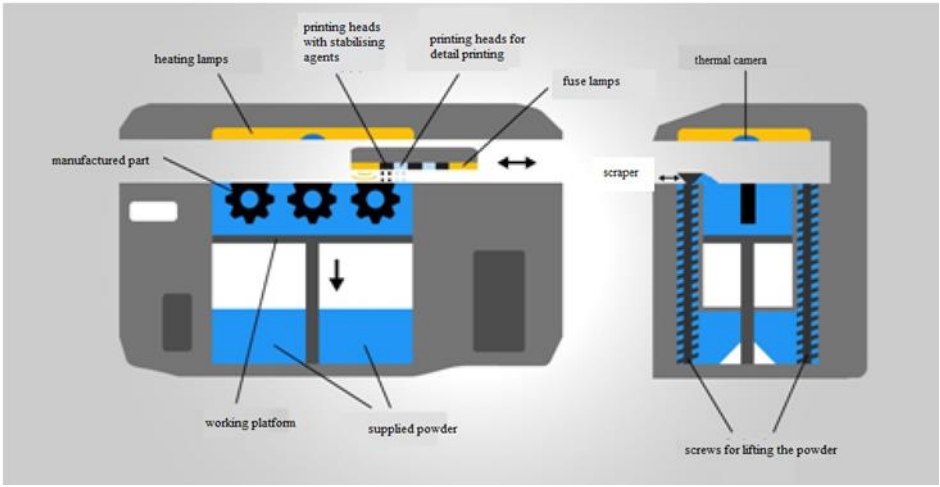

Fig. 1. The principles of MJF method [3]

Fig. 2. Comparison of quality of the obtained external surfaces
From left: CNC machining, FDM technology and MJF technology [4]

2. PREPARATION OF MATERIAL SAMPLES FOR TESTING

The method of carrying out the plastic tensile test is described in standard PN-EN ISO 527: 1998 Plastics – Determination of tensile properties (according to which the tests were performed). The three-dimensional model of the sample for strength tests was modelled using the SolidWorks program. Figure 3 shows the appearance of the broken sample, while Table 1 shows all its geometrical dimensions.

The samples were made of polyamide PA12 in two printing modes, which have a direct impact on the density of the internal structure of the sample and its production time. In Balance mode the sample had a much more bonded structure as opposed to the printing of samples in Fast mode, where the internal structure of the sample is less bonded with a fusing agent. This, in turn, has an impact on the strength of the samples and their production times.

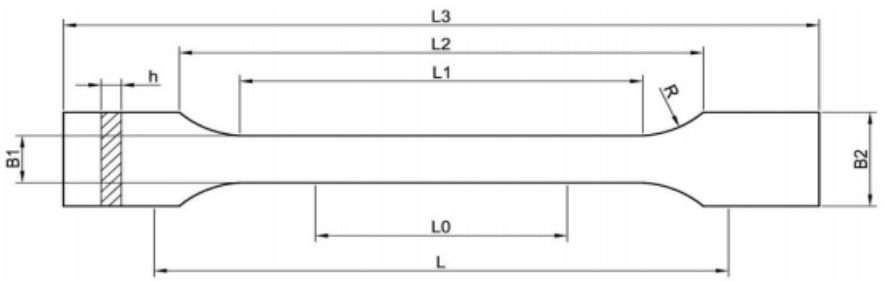

Fig. 3. Sample intended for strength tests [5]

Table 1. Sample dimensions [6]

Sample dimensions	Dimension
L3- overall length	150 mm
L1- length of part limited by lines	40 mm
R- radius	60 mm
L2- distance between the wide parallel parts	106 mm
B2- width at ends	20 mm
B1- width of the narrow part	10 mm
H- thickness	4 mm
L0- measurement length	50 mm
L- initial distance between grips	115 mm

To obtain the strength parameters, a hybrid test stand was used – an INSTRON 5967 universal testing machine controlled by the Bluehill 3 program and coupled with the ARAMIS measurement system (GOM, Gmbh), enabling the monitoring of deformations in three axes [7]. For this purpose, the samples were properly prepared by matting them and applying a characteristic pattern (Fig. 4). Measurements were made at 23°C and 55% humidity with a stretching rate of 5 mm/min. 1 measurement series consisted of 6 samples.

Fig. 4. Samples with a white pattern for testing with the use of digital image correlation (DIC) [8] [own study]

2. RESULT ANALYSIS

Based on the photos taken, the material constants (Poisson's ratio and Young's modulus) were determined in the range of elastic deformations of 0.05-0.25% using the Aramis system and the deformation fields in the X and Y axes at the moment of the maximum breaking force were characterised. The results obtained of material data are presented in Table 2.

Table 2. Summary of test results for static tensile test of printed samples in FAST and BALANCE mode [own study]

Sample name	F [kN]	σ [MPa]	e [%]	Rp02 [MPa]	v [-]	mE [MPa]
FAST	1.26±0.21	32.2±5.4	4.12±1.09	20.0±0.8	0.406±0.003	1570±58
BALANCE	1.38±0.19	36.3±5.3	3.26±0.09	22.5±0.8	0.395±0.023	1797±48

F – load at break, σ – breaking stress, e – strain at break, Rp02 – proof stress, v – Poisson's ratio, mE – Young's modulus, ± – standard deviation

Figures 5-8 show representative graphs generated during the tests, on the basis of which the conventional yield point (Rp02), Poisson's ratio (v) and Young's modulus (mE) were determined.

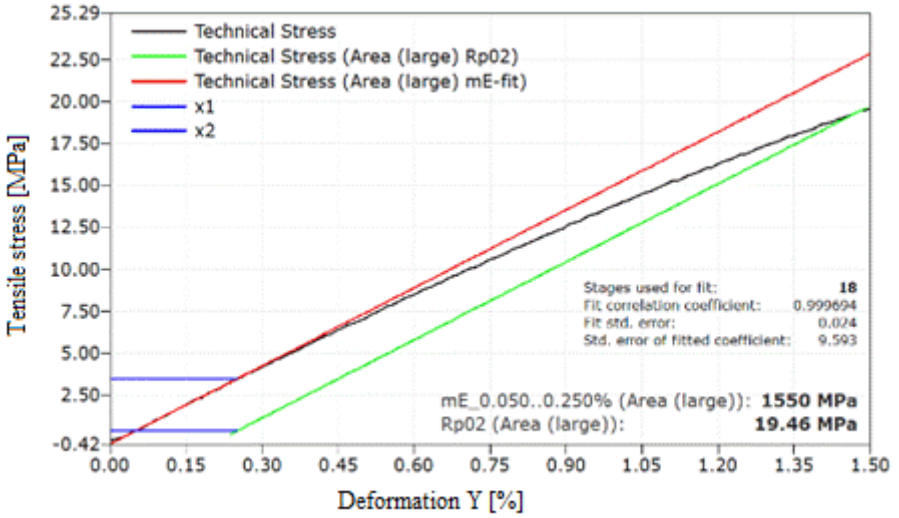

Fig. 5. A representative diagram of the tensile stress – longitudinal strain Y correlation in the elastic range with determination of Young's modulus and yield stress for the FAST_2 sample (i.e. sample 2 printed in Fast mode)

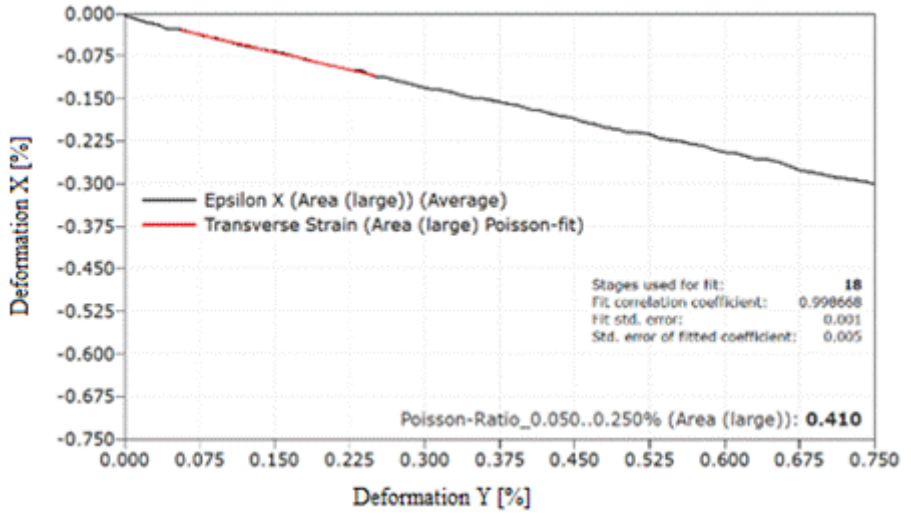

Fig. 6. A representative diagram of the transverse deformations X – longitudinal deformations Y correlation in the elastic range with determination of the Poisson's ratio for the FAST_2 sample (i.e. sample 2 printed in Fast mode)

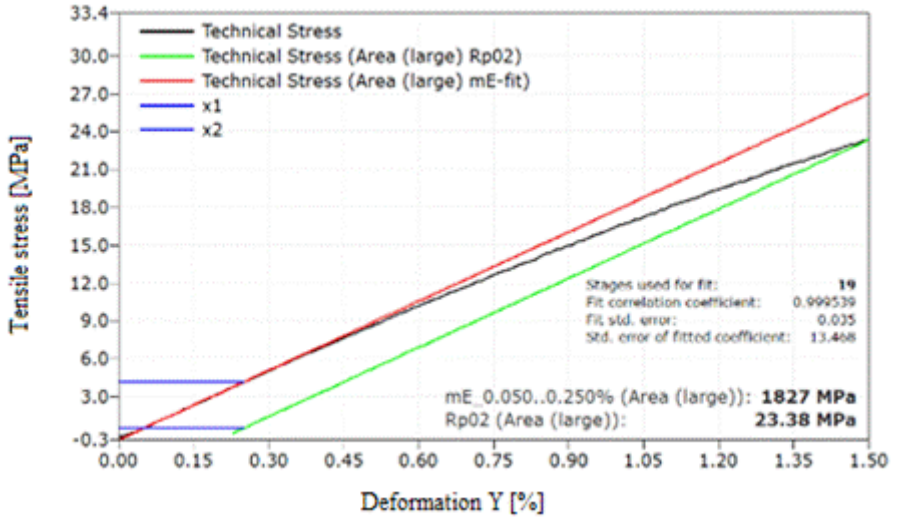

Fig. 7. A representative diagram of the tensile stress – longitudinal strain Y correlation in the elastic range with determination of Young's modulus and yield stress for the BCE_1 sample. (i.e. sample No. 2 printed in Balance mode)

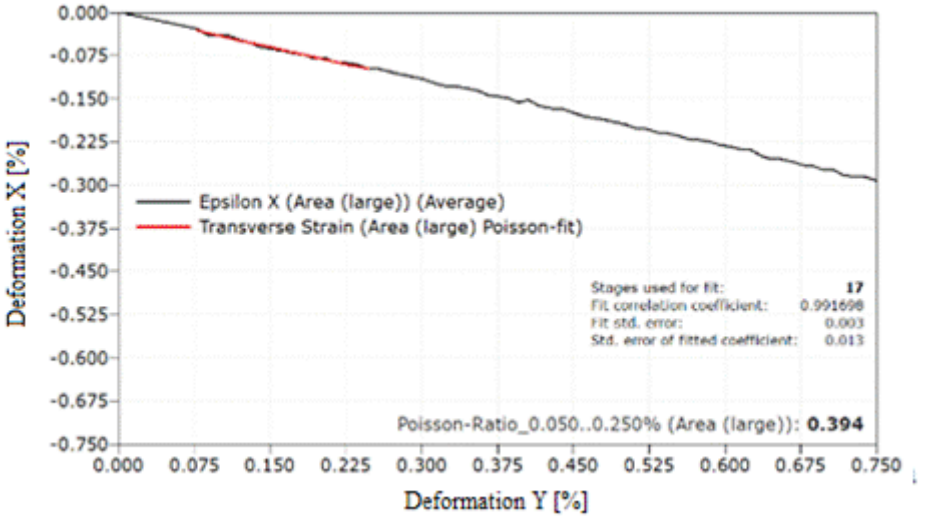

Fig. 8. A representative diagram of the transverse deformations X - longitudinal deformations Y correlation in the elastic range with determination of the Poisson's ratio for the BALANCE_2 sample (i.e. sample No. 2 printed in Balance mode)

Based on the photos taken during sample stretching, an analysis of local deformations on their surfaces was also carried out. Figures 9-14 show the representative characteristics of deformations in the X and Y axes recorded at the maximum breaking force and the moment of breakage for representative samples.

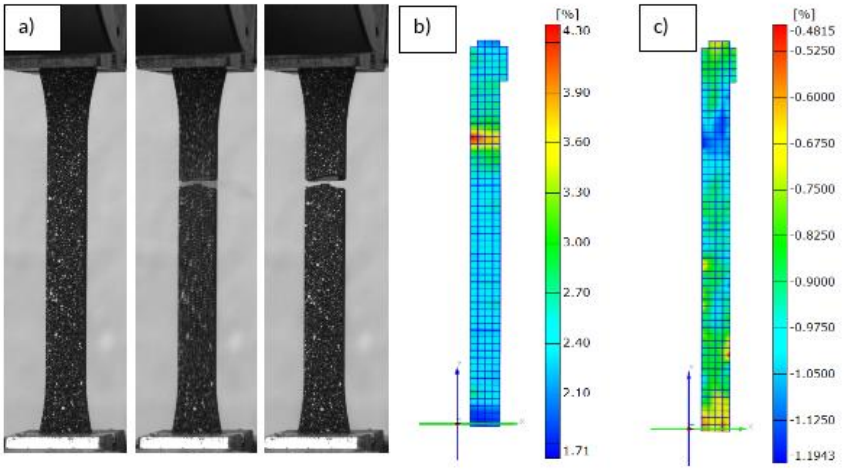

Fig. 9. The sample moment of breakage (a) and the deformation field under the influence of the maximum force in the direction of the Y (b) and X (c) axes for the FAST_4 sample (σ = 24.33 MPa, e = 2.56%) [own study]

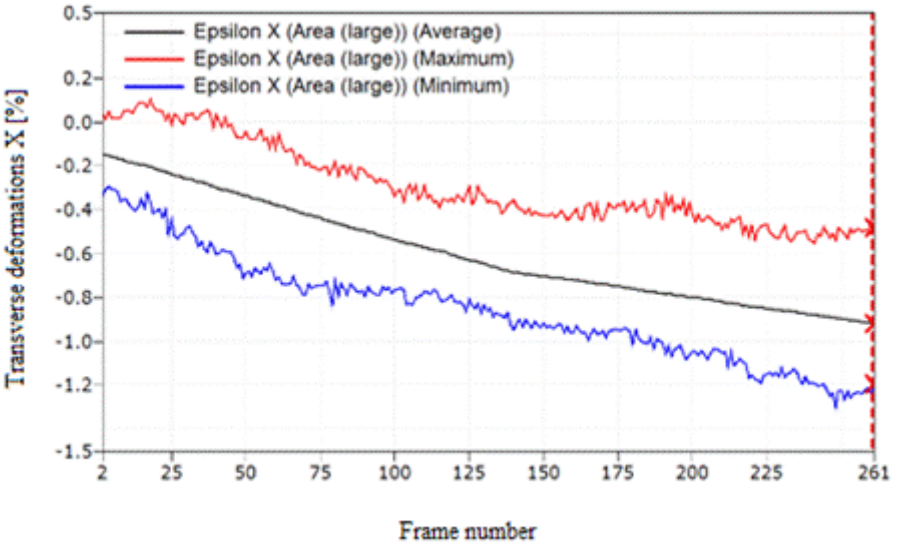

Fig. 10. The distribution of deformations in the transverse direction X during the stretching of the FAST_4 sample, recorded in the scope of longitudinal deformations 0.41-2.56% [own study]

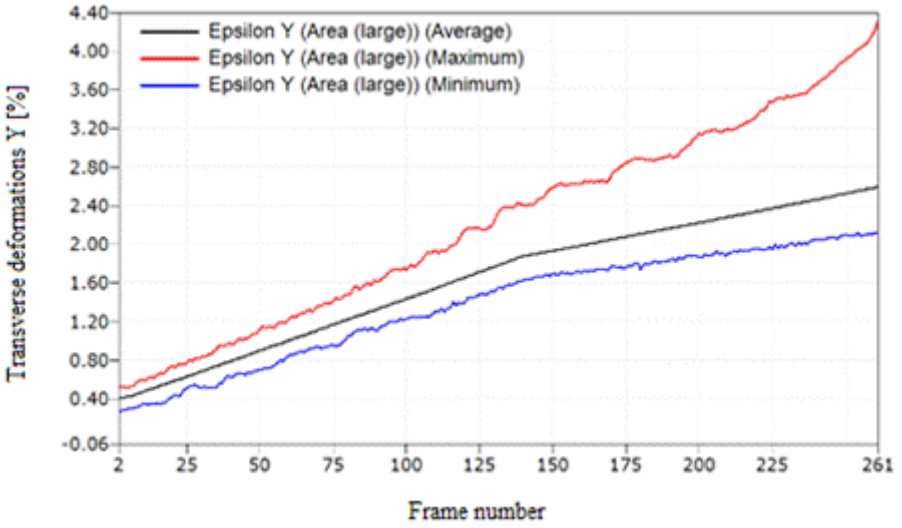

Fig. 11. The distribution of deformations in the longitudinal direction Y during the stretching of the FAST_4 sample, recorded in the scope of stretching deformations 0.41-2.56% [own study]

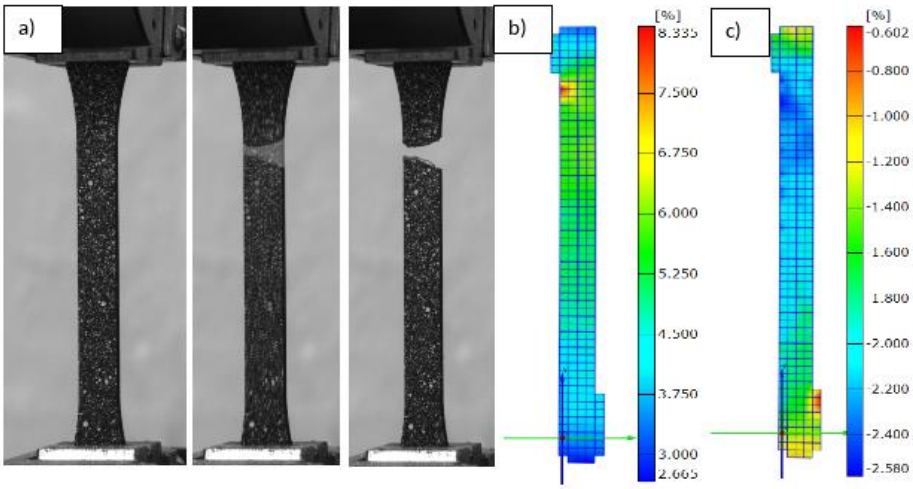

Fig. 12. The sample breaking moment (a) and the deformation field under the influence of the maximum force in the direction of the Y (b) and X (c) axes for the FAST_5 sample (σ = 34.83 MPa, e = 5.02%) [own study]

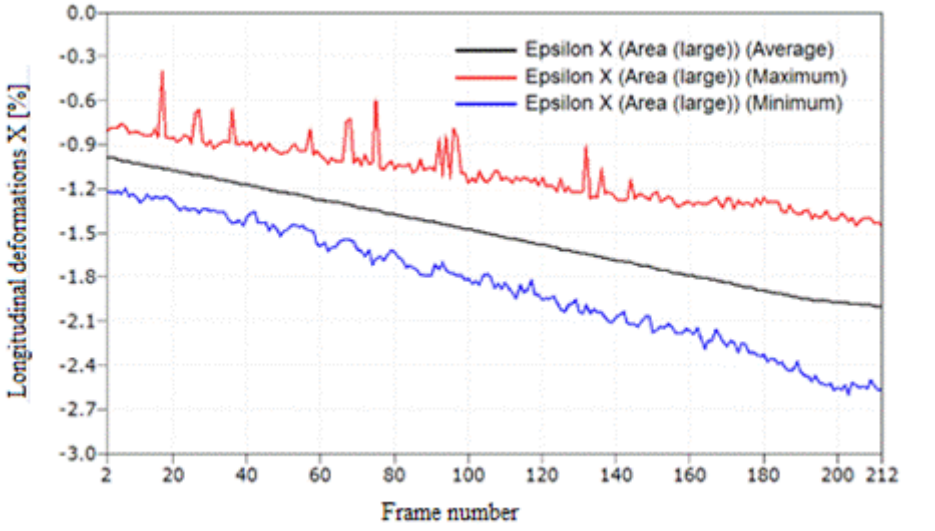

Fig. 13. The distribution of deformations in the transverse direction X during the stretching of the FAST_5 sample, recorded in the scope of longitudinal deformations 2.51-5.01% [own study]

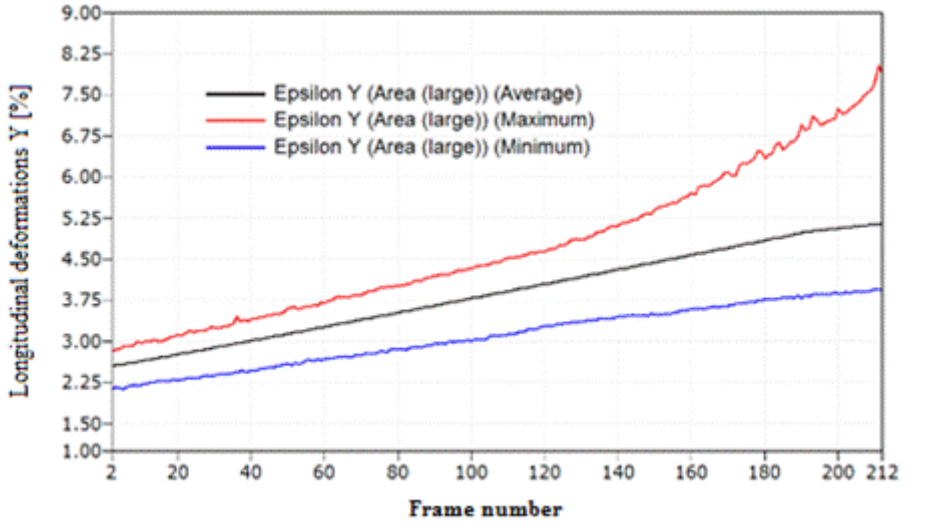

Fig. 14. The distribution of deformations in the longitudinal direction Y during the stretching of the FAST_5 sample, recorded in the scope of stretching deformations 2.51-5.01% [own study]

4. CONCLUSIONS

The results obtained indicate that samples printed in BALANCE mode have greater stiffness and strength, which is the result of the way these samples are built in both modes. As a result, they also have less deformations when broken. In turn, a more detailed analysis of the deformation fields in the direction of the Y and X axes shows that at the moment of breakage:

a) for FAST samples:
- the maximum local deformations in the direction of the Y axis are within the range of 1.71 ÷ 4.30 and 2.66 ÷ 6.33%,
- the maximum local deformations in the direction of the X axis are within the range of -0.26 ÷ (-0.60)% and -1.19 ÷ (-0.48)%,

b) for BALANCE samples:
- the maximum local deformations in the direction of the Y axis are within the range of 1.86 ÷ 6.61 and 6.38 ÷ 12.72%,
- the maximum local deformations in the direction of the X axis are within the range of -1.82 ÷ (-0.20) and -5.96 ÷ (-2.00)%.

Due to the fact that the technology has been present for only 4 years, knowledge about it is mostly empirical; it is familiar only to the people closely related to this technology. There are no published results of scientific research on the relationship between individual parameters and their impact on the overall effect in the form of print quality.

FUNDING

The research was carried out as part of subsidised projects titled: "3D printing products prepared for advanced applications in the machine industry" co-financed by the European Regional Development Fund under priority axis I "The use of research and development activities in the economy" and as part of: Measure 1.2 "Research and development activities of enterprises" of the Regional Operational Programme of the Mazowieckie Voivodeship for 2014-2020.

REFERENCES

[1] Kiński Wojciech, Paweł Pietkiewicz. 2017. "Główne parametry eksploatacyjne wpływające na jakość wydruków w technologii FDM". *Przegląd Mechaniczny* 6 : 54-56.

[2] Wittkopf A. Jarrid, Kris Erickson, Paul Olumbummo, Aja Hartman, Howard Tom, Lihua Zhao. 2019. 3D Printed electronics with Multi Jet Fusion. In *NIP & Digital Fabrication Conference* 1 : 29-33.

[3] http://www.tth.com/, (access on 28.07.2020).
[4] http://www.hp3d.pl/, (access on 12.08.2020]
[5] Miazio Łukasz. 2015. „Badanie wytrzymałości na rozciąganie próbek wydrukowanych w technologii FDM z różną gęstością wypełnienia". *Mechanik* 7 : 533-538.
[6] Kiński Wojciech, Paweł Pietkiewicz. 2019. "Influence of the print layer height in FDM technology on the rolling force value and the print time". *Agricultural Engineering* 23(4) : 1-9.
[7] Oliwa Rafał. 2015. Zastosowanie systemu ARAMIS do trójwymiarowego pomiaru lokalnych odkształceń kompozytów. W *Materiały konferencyjne I Krajowej Konferencji Naukowej Szybkie prototypowanie: Modelowanie-Wytwarzanie-Pomiary*, 147-151, 16-18.09.2015, Rzeszów-Pstrągowa.
[8] Golewski L. Grzegorz. 2011. „Zastosowanie systemu Aramis w badaniach odporności na pękanie kompozytów betonowych modyfikowanych dodatkiem popiołów lotnych". *Kompozyty* 11(1) : 3-8.

Wpływ zmiany parametrów procesu Multi Jet Fusion (MJF) na wytwarzane obiekty przestrzenne

Maciej CADER[1], Wojciech KIŃSKI[2]

[1]*Sieć badawcza Łukasiewicz - Przemysłowy Instytut Automatyki i Pomiarów PIAP*
al. Jerozolimskie 202, 02-486 Warszawa
[2]*Uniwersytet Warmińsko-Mazurski w Olsztynie, Wydział Nauk Technicznych*
ul. Michała Oczapowskiego 1, 10-719 Olsztyn

Streszczenie. W artykule szczegółowo omówiono zasadę działania technologii Multi Jet Fusion. Przeprowadzone zostały hybrydowe badania wytrzymałościowe maszyną wytrzymałościową typu INSTRON 5967 sterowaną za pomocą programu Bluehill 3 oraz sprzężoną z systemem pomiarowym ARAMIS (GOM, Gmbh), umożliwiającym monitorowanie odkształceń w trzech osiach, przy wykorzystaniu systemu szybkich kamer. Przedstawione zostały wyniki badań testu statycznej próby rozciągania próbek w dwóch charakterystycznych dla technologii MJF trybach drukowania – z ang. FAST i z ang. BALANCE.
Słowa kluczowe: drukarka 3D, analiza wytrzymałościowa, MJF